Journal of Rehabilitation in Civil Engineering 8-4 (2020) 73-89

journal homepage: http://civiljournal.semnan.ac.ir/

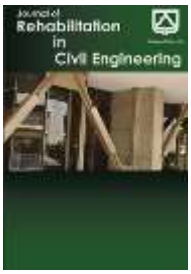

Experimental Investigation of Mechanical and Dynamic Impact Properties of High Strength Cementitious Composite Containing Micro Steel and PP Fibers

A. Dalvand[1*], E. Sharififard[2] and F. Omidinasab[3]

1. Assistant Professor, Department of Engineering, Lorestan University, Khorramabad, Iran
2. Graduated MS of Marine Structural Engineering, Department of Civil and Environmental Engineering, Amirkabir University of Technology, Tehran, Iran
3. Assistant Professor, Department of Engineering, Lorestan University, Khorramabad, Iran

Corresponding author: *dalvand.a@lu.ac.ir*

ARTICLE INFO

Article history:
Received: 20 March 2019
Accepted: 24 June 2020

Keywords:
Cementitious composites,
Mechanical properties,
Impact resistance,
High strength.

ABSTRACT

Cementitious composites are one of the most consumed construction materials in the world. The use of cementitious composites is increasing due to their special characteristics. The behavior of high strength cementitious composites is improved by increasing the fiber percentage. In the present paper, the effects of steel microfibers and polypropylene fibers on mechanical properties and impact resistance of high strength cementitious composites are investigated. The percentage of fibers used in the study was 0, 0.5, and 1.5% in seven separate and three combined mix designs. Experiments were carried out on 120 specimens in 10 mix designs. Compressive strength, tensile strength, flexural strength, and dynamic impact tests were carried out on 10 mix designs manufactured in this research. The dynamic impact strength of the disc specimen was investigated by a drop hammer test machine with a capacity of 7500J. After testing the samples, it was shown that using a high percentage of steel and polypropylene fibers reduces the compressive strength and increases tensile strength, flexural strength, and impact strength. The effects of steel microfibers on the reduction of the crush displacement resulting from the dynamic impact were higher than that of polypropylene fibers.

1. Introduction

With the increase in population and the need for structures, demand for concrete has grown considerably as one of the main building materials. In this light, various cementitious materials have been developed. To improve the mechanical properties of

DOI: 10.22075/JRCE.2020.17480.1332

concrete, additives such as fibers are used in concrete. In recent years, high strength cementitious composites have been widely used around the globe. The term "high strength" refers to composites with strength above 42 Mpa [1-2]. In the construction industry, high strength concrete has been considered for prestressed products, prestressed structures, columns, and concrete shear walls in tall buildings and specially for connecting precast members such as bridge decks [3-5]. One of the limitations of using high strength concrete is its higher brittleness compared to the normal concrete [6]. The high ductility of cementitious composites attracted the attention of researchers [7]. Adding fiber to composite reduces brittleness [8]. In cementitious composites, fibers can increase many engineering properties such as flexural strength, failure toughness, thermal resistance, impact resistance under dynamic impact loads, and fatigue strength [9, 10]. The use of fibers in the concrete reduces the velocity of crack propagation and increases the ductility. Some of these fibers include steel, carbon, glass, and polymer. Fiber concrete has good properties such as ductility, high energy absorption, crack resistance and stiffness [11]. In the 1960s, Romualdi et al. investigated the effects of steel fibers on the reduction of concrete fragility [12]. This positive effect was iterated with the use of other types of fibers, and in recent years, a combination of fibers with different lengths has been studied [13]. Increased knowledge of how the fibers affect the mortar led to recommendations for structural design by the RILEM Institution [14]. Engineering Cementitious Composite (ECC) was first developed at the University of Michigan [15]. Due to the formation and propagation of multiple cracks in ECC composites, tensile ductility has considerably improved [16]. In these cementitious composites, the amount of fiber has reduced to less than 2%. According to studies from 1993 to 2003, tensile strengths of 4 to 6 MPa and tensile ductility of 3 to 5% have been observed in these composites. Engineering composites have a wide range of applications, one of which is in self-compacting cementitious composites on a large scale and compression reinforcement [17, 18]. Cementitious composites with high initial strength are other types of these composites which are used in structures that require rapid growth of initial strength [19]. There is also a type of engineering cementitious composites that are used in lightweight structures with a low specific weight [20]. Another type of environmentally friendly cementitious composite has also been made [21]. Another type of engineering cementitious composite is being developed which has self- healing properties. In other words, these types of composites are used to restore the mechanical properties of materials after damage [21]. The use of concrete and cementitious composites is increasing due to advantages such as high compressive strength, corrosion resistance, high energy absorption against impact loads, and cost-effectiveness. The behavior of materials must be determined in the design of structures. The static method is used in conventional concrete loading. In the static method, the loading rate on the specimens is low. Concrete and all types of cementitious composites are sensitive to the velocity of load application [22]. The micro steel fibers are widely used to produce self –compact composites [23]. This type of fibers have a length of less than 30mm and aspect ratio more than 64. Also, micro steel fibers are suitable to cast of prefabricated concrete parts [24]. As well as, with attention to this

point that the micro steel fibers have a great ability to absorption of impact dynamic force, studying about characteristics of it, is very necessary [25]. A geopolymer binder is an alternative cementitious material and it is produced by the polymerization of aluminosilicate materials by an alkali solution [26]. Using some fibers such as steel and polypropylene fibers as a new composition were developed by many researchers in recent years. By adding steel and polypropylene fibers to the alkali-activated binder composition, the mechanical properties of this materials were improved [24, 27]. The use of static loading alone could not be a good response to the behavior of the concrete and cementitious composites against impact loads. Using the fibers can be increased the energy absorption of composite specimens. In this research, high strength cementitious composite specimens with different percentages of steel microfiber and PP fibers were manufactured and tested. The effects of combination of micro steel fibers and PP fibers and their mechanical properties are investigated in dynamic impact tests.

2. Materials and Concrete Mix Design

To make the mix designs, the Portland cement, Type 2, was used in accordance with ASTM C150 [28]. Table 1 shows the chemical and physical properties of the cement used in the present study. They specific gravity of them were 2650Kg/m3. Also, the water absorption of fine aggregate was 0.69%. Also, for the determination of water absorption of fine aggregate, a water absorption test was performed on fine aggregate according to AASHTO T84 [29]. A viscosity modifying material was used to make the cementitious composite. Also, to reduce water consumption and increase the workability of cementitious composites, a superplasticizer named Dezobuild D-10 was used. In this study, micro steel fibers and polypropylene fibers were used. The properties of the fibers used are provided in Table 2. Also, a schematic of the fibers used is shown in Fig 1. In manufacturing the specimens of the study, the fibers were added to the mix at the final stage, and endeavor was made to distribute the fibers uniformly in the sample. First, the sand and cement were mixed in a mixer, and then 90% of water was added. Finally, 10% of remaining water was added to the mix after mixing with the superplasticizer. Ten mix designs used in the manufacture of cementitious composites are presented in Table 3. Also, The amount of consumed water, cement, and aggregates for all mix designs were selected 370, 980 , 1420 Kg/m3 , respectively. As well as, the water to cement ratio was 0.38 for all mix designs.

Table 1. Chemical composition and physical properties of Portland cement.

Composition	(%)
SiO_2	21.1
Al_2O_3	4.37
Fe_2O_3	3.88
MgO	1.56
K_2O	0.52
Na_2O	0.39
CaO	63.33
C_3S	51
C_2S	22.7
C3A	5.1
C_4AF	11.9
Physical properties	
Specific gravity	3.1
Specific surface ($\frac{Cm^2}{gr}$)	3000

Table 2. Mechanical properties of fibers.

Fiber Type	Length (mm)	L/D	Tensile stress (MPa)	Elastic module (GPa)	Density (Kg/m^3)
Micro Steel	10 to20	20 to 150	240	200	7850
Polypropylene	6	--	400	3.5-3.9	910

Fig. 1. Micro Steel and Polypropylene fibers.

Table 3. The mix compositions (kg/m^3).

Mix designs	W/C	Water ($\frac{Kg}{m^3}$)	Cement ($\frac{Kg}{m^3}$)	Aggregates ($\frac{Kg}{m^3}$)	Fiber Volume (%)		SP
					Micro Steel	PP	
S0PP0	0.38	370	980	1420	0	0	4.9
S.5PP0					0.5	0	
S1PP0					1	0	
S1.5PP0					1.5	0	
S0PP.5					0	0.5	
S0PP1					0	1	
S0PP1.5					0	1.5	
S.5PP.5					0.5	0.5	
S.5PP1					0.5	1	
S1PP.5					1	0.5	

3. Procedure of Experimental Tests

3.1. Compressive and Split Tensile Tests

The compressive strength test was performed on cubic specimens with side lengths of 100 mm in accordance with ASTM C39 [30] with a loading rate of 0.3 MPa/s. In this test, a digital compression testing machine, capacity 1000KN, was used. Moreover, the splitting tensile strength test, in accordance with ASTM C496 [31], was performed on the cylindrical specimens with 100mm of diameter and 200mm of height at a loading rate of 0.05 MPa/s [32]. The tensile strength

of splitting test was calculated by the following equation:

$$\sigma_{xx} = \frac{2P}{\pi LD} \quad (1)$$

Where, D is the diameter and L the length of cylindrical samples, and P is the maximum load applied.

3.2. Flexural Three Point Bending Tests

The three-point bending test (the application of a concentrated load at mid-span), in accordance with ASTM C1609 [33], was performed on 30 bending beams measuring

The applied flexural force was measured by a load cell with a capacity of 100 KN, and the deflection of beams was measured by LVDT, 150 mm long.

3.3. Impact Tests

To investigate the effects of dynamic impact loading on cementitious composites, disc specimens with the height of 65 mm and diameter of 150 mm were constructed in accordance with Fig. 2a. Impact loading was performed on composite specimens with varying fiber content. This type of loading was performed to determine parameters such as initial peak force, crush displacement and energy absorption. The impact test results of the specimens were compared by the 7500 j drop hammer test machine (DH-TM-7500J). The DH-TM-7500J machine has a falling height of 3m and a hammer weight of 180 to 250 kg (Fig. 2b). This machine has three semispherical hammer heads for the comparison of the results of the deformation of the specimens during impact (Fig. 2c). Data were taken and processed by an accelerometer sensor with the precision of microseconds.

320 mm long, 60 mm wide, and 80mm high. Fig. 5 shows the way the test was performed.

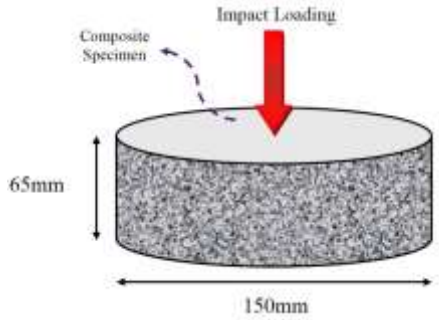

a)

b)

c)

Fig. 2. a. Sample of the constructed disc, b. Semispherical hammer head, c. 7500J drop hammer test machine (DH-TM-7500J).

4. Results and Discussion

4.1. Compressive Strength

In Fig 3, the compressive test machine is shown. The presence of PP fibers in cement paste results in the formation of a water film at the interface of the fiber and matrix called wall effect. Due to the greater mobility of calcium ions in a water environment, portlandite (calcium hydroxide) macro crystals can easily grow and make the transition zone more porous [34]. This phenomenon has a negative effect on the bond between PP fiber and matrix. In this regard, it seems that addition of PP fibers could not have significant improvement on mechanical properties of the cementitious specimens. Therefore, it is clear that to utilize the maximum strength of the fiber and improve the composite properties, it is essential to enhance the interfacial bond of PP fibers. Some studies have shown that effectiveness of fibers is significantly affected by chemical fiber-to-matrix adhesion [35]. According to the results of Table 4, the highest compressive strength is related to the S1PP0 group (with 1% steel microfiber). The compressive strength of the S1PP0 group with 1% steel fibers is 12% higher than the S0PP1 group with 1% PP fibers. Also, the strength of S1PP0 and S0PP1 groups were 22% and 11% higher than the S0PP0 (no fibers) group, respectively. As shown in Fig. 4, the effect of steel fibers on compressive strength is higher than that of PP. Increasing the percentage of steel fibers from 1 to 1.5% decreased the compressive strength by 7%. Also, increasing the percentage of steel fibers from 1 to 1.5% decreased the compressive strength by 9%.

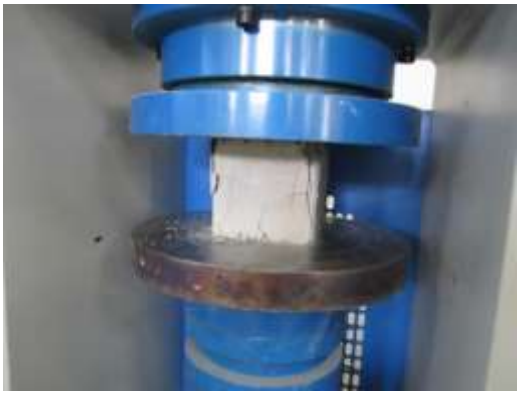

Fig. 3. Compressive test machine.

Table 4. Summary of experimental results obtained from compressive tests.

Number	Mix designs	Fibers(%)		Compressive Strength (MPa)
		Steel	PP	
1	S0PP0	0	0	67.18
2	S.5PP0	0.5	0	73.51
3	S1PP0	1	0	82.11
4	S1.5PP0	1.5	0	76.29
5	S0PP.5	0	0.5	69.91
6	S0PP1	0	1	74.42
7	S0PP1.5	0	1.5	68.11
8	S.5PP.5	0.5	0.5	75.73
9	S.5PP1	0.5	1	74.21
10	S1PP.5	1	0.5	78.37

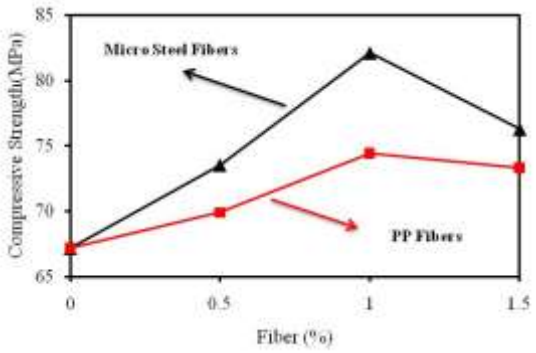

Fig. 4. Effects of fibers in compressive strength.

4.2. Splitting Tensile Strength

Fig. 5 shows the method of tensile strength test. Table 5 shows the results of the tensile test performed on the samples. Increasing the amount of fibers has increased tensile strength. The tensile strength of the specimens reinforced with fibers is significantly higher compared to those without fibers. The maximum tensile strength in the specimens is related to the group S1.5PP0, in which, the tensile strength is 55% higher than the S0PP1.5 group. As shown in Table 5, the effect of adding micro steel fibers on tensile strength is greater than that of polypropylene fibers. With the addition of 0.5, 1, and 1.5% of the steel fibers, the tensile strength is, respectively, 85, 130 and 186% higher than the specimens without fibers. Also, with the addition of 0.5, 1, and 1.5% of the PP fibers, the tensile strength is, respectively, 29, 57 and 65% higher. In the specimens with composite fibers, the effects of steel fibers are far more than PP fibers. In the S.5PP.5 group, the tensile strength increased by 6 and 33% compared to the S.5PP0 and S0PP.5 groups. Table 5 represents a comparison between experimental tensile strengths, the results of regulatory design codes, and the literature. As can be seen in Table 5, in specimens with steel and polypropylene fibers, the difference between experimental results and other computations is high. This difference results from the fact that the effects of fibers were not taken into account in calculations.

4.3. Flexural Strength

In this research, the flexural strength of composite mix designs was calculated according to ASTM C1609 [33]. Flexural strength test was carried out on ten different mix designs of beams containing steel micro fibers, PP fibers, and a combination of these. An illustration of the method of performing the experiment and the dimensions of the specimen are shown in Fig. 6. Also, in the column diagram of Fig. 7, the flexural strength values obtained from the experimental results are shown. According to the figure, the maximum flexural strength is related to the S1.5PP0 group. The flexural strength of the S1.5PP0 group is 74, 166, and 19% higher than the S0PP0, S.5PP0, S1PP0 groups, respectively. Also, in groups with PP fibers, flexural strength increased with the increase in the fiber content. The S0PP1.5 group had the highest flexural strength among the groups with PP fibers, the bending strength of which was 39, 21, and 10% higher than S0PP0, S0PP.5 and S0PP1 groups, respectively.

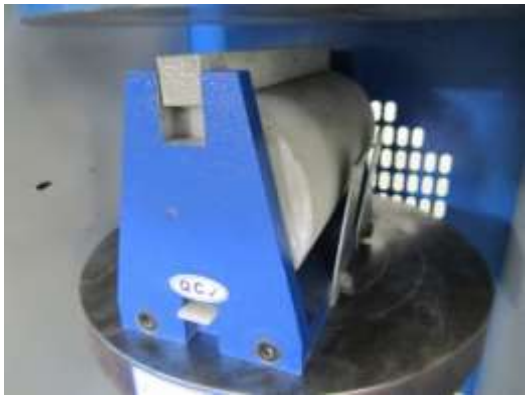

a)

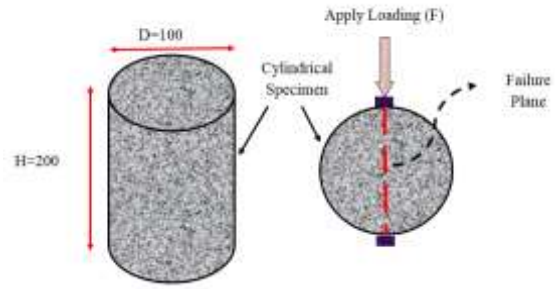

b)

Fig. 5. Splitting test setup a) Test Machin b) Dimention of splitting test specimen.

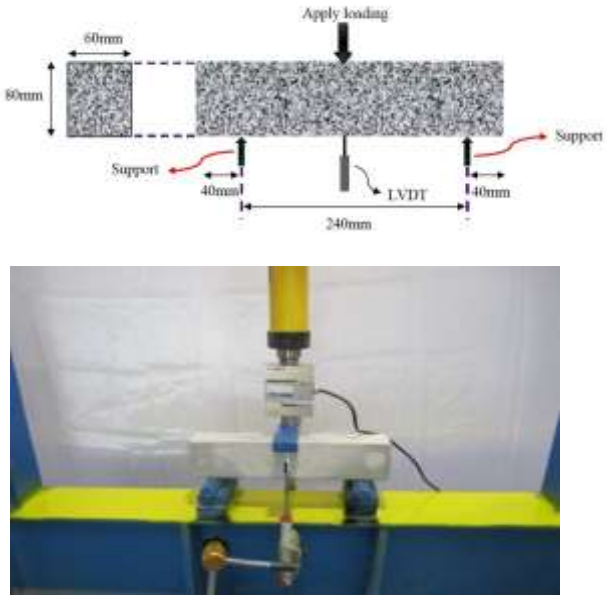

Fig. 6. Three point bending test setup.

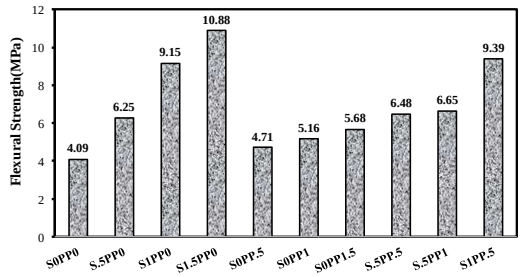

Fig. 7. Flexural strength of all mix designs.

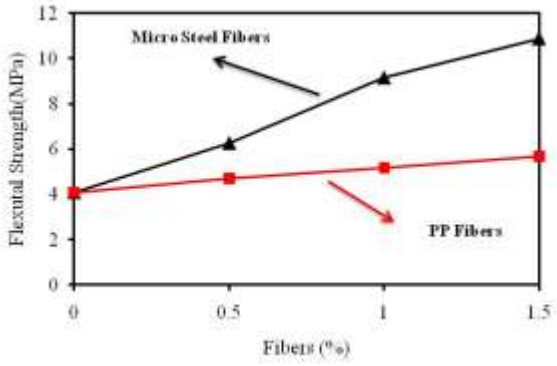

Fig. 8. Changing flexural strength versus fiber percentage.

Fig. 8 shows how flexural strength changes in terms of the percentage of micro steel and PP fibers. As seen in the figure, with the increase in the steel fibers contents from 0 to 0.5%, the flexural strength increased from 4.09MPa to 10.88MPa. Meanwhile, with the addition of PP fibers, the flexural strength was increased from 4.09MPa to 5.68MPa. The slope of the increase in flexural strength in terms of fiber content is higher for steel fibers than PP fibers.

4.3.1. Toughness Index

In Fig 9, the load-displacement curve for the mid-span of the flexural samples is presented. As shown in Figure 9, the behavior of the curve changes with the increasing fiber percentages. According to Fig 9, the presence of micro steel fibers in the composition, as compared to PP fibers, has increased the capacity of changing the displacement capacity of samples. The initial slope of the specimens is approximately similar.

Until 2006, researchers calculated the flexural toughness according to the ASTM C1018 standard. According to this standard, displacement corresponding to the formation of the first cracks should be determined. Because of the difficulties in exact determining of the parameter, this standard became obsolete after 2006. In recent years, the ASTM C1609 standard is used instead of the standard ASTM C1018 to determine the flexural toughness. In this research, both ASTM C1018 and ASTM C1609 standards have been used to determine the flexural toughness. Results are analyzed using both methods. In order to determine the flexural toughness according to the ASTM C1018 standard, toughness indexes including I_5, I_{10}, I_{15}, I_{20} are determined based on the characteristic points specified on the load-displacement curve shown in Fig 10 and according to the Equation (2).

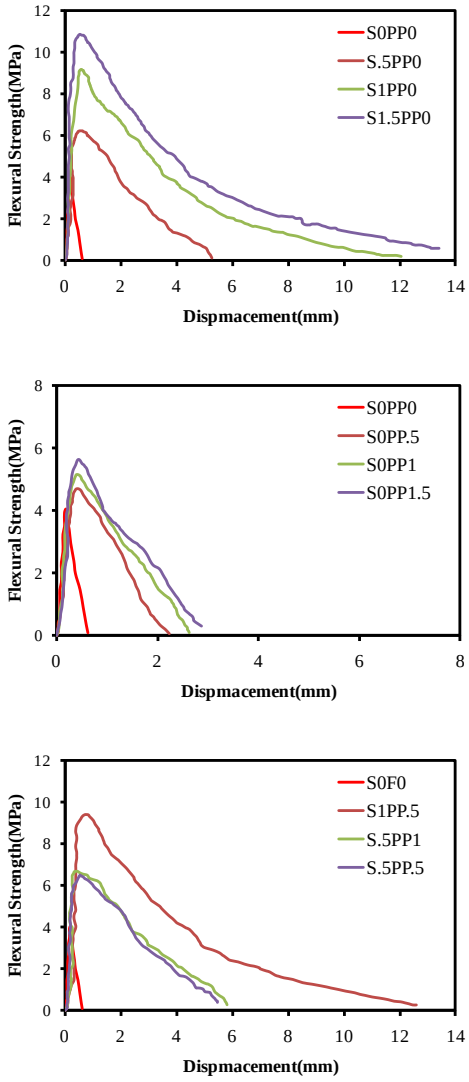

Fig. 9. Load-displacement curve of flexural mix designs.

$$I_5 = S_{OACD}/\ S_{OAB}$$
$$I_{10} = S_{OAEF}/\ S_{OAB}$$
$$I_{10} = S_{OAGH}/\ S_{OAB} \quad (2)$$
$$I_{15} = S_{OAMN}/\ S_{OAB}$$

In equation (1):

S_{OAB} → the area under a load-displacement curve in displacement corresponding to the first crack

S_{OACD} → the area under a load-displacement curve in displacement which is 3 times more than displacement corresponding to the first crack

S_{OAEF} → the area under a load-displacement curve in displacement which is 5.5 times more than displacement corresponding to the first crack

S_{OAGH} → the area under a load-displacement curve in displacement which is 10.5 times more than displacement corresponding to the first crack

S_{OAMN} → the area under a load-displacement curve in displacement which is 15.5 times more than displacement corresponding to the first crack

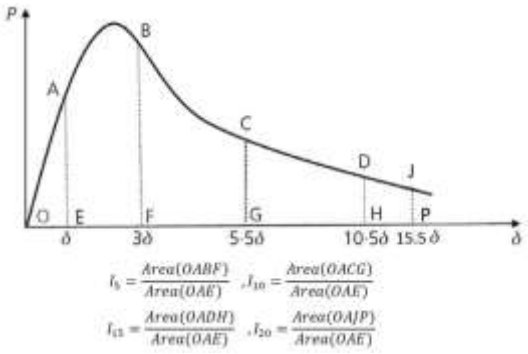

Fig. 10. Definition of flexural toughness indices based on ACTM C1018.

In order to compare the flexural strength of the specimens according to the ASTM C1609 standard, the flexural toughness is obtained from the surface below the load-displacement curve to the displacement of L/150, where L is the span length of loading(L=240mm) in the beam specimen and the flexural strength coefficient is calculated according to Equation (3).

$$R^{D}_{T,150} = \frac{150T^{D}_{150}}{f_1\ b\ d^2} \quad (3)$$

In the Equation (3), $R^{D}_{T,150}$, the coefficient of flexural strength, T^{D}_{150}, the degree of flexural toughness up to the corresponding point L/150 in terms of Joule (J), f_1 is rupture modulus (stress corresponding to the first crack) in terms of MPa, and b and d are the width and height of the sample in terms of

mm(b=60mm and d=80mm). In the table 6, the rupture module, flexural toughness of the specimens for the equivalent displacement (L/150) and the flexural strength coefficient are calculated and shown according to the ASTM C1609. It can be seen that steel fibers can increase the rupture modulus of flexural specimens significantly. By increasing the fibers, the flexural strength of the sample will be increased because these fibers have high tensile strength and bridge on the cracks in the tensile region. However, the PP fibers could not increase rupture module significantly. Table 6 shows the indexes of toughness according to ASTM C1018 standard. The results also indicate that micro steel fibers can increase the toughness indices in this standard, which is considerably higher than PP fibers specimens.

Table 5. Splitting tensile strength of cylindrical specimens.

Mix designs	Compressive strength (MPa)	Splitting strength(MPa)							
		Experimental	ACI Committee 318 (2014)	CEB-FIB (1991)	Carino and Lew (1982)	Oluokum et al (1991)	Artoglu et al (2006)	Lavanya and jegan (2015)	Gardner (1990)
			$0.56f_c^{'0.5}$	$0.3f_c^{'0.66}$	$0.272f_c^{'0.71}$	$0.294f_c^{'0.69}$	$0.387f_c^{'0.6}$	$0.249f_c^{'0.772}$	$\mathbf{0.33f_c^{'0.}}$
S0PP0	67.18	3.18	3.81	4.38	4.87	4.85	5.00	5.73	4.96
S.5PP0	73.51	5.87	3.99	4.65	5.19	5.16	5.29	6.14	5.26
S1PP0	82.11	7.32	4.21	5.00	5.61	5.57	5.68	6.69	5.67
S1.5PP0	76.29	9.11	4.06	4.76	5.33	5.29	5.42	6.32	5.40
S0PP.5	69.91	4.09	3.89	4.50	5.01	4.98	5.13	5.91	5.09
S0PP1	74.42	4.98	4.01	4.69	5.23	5.20	5.34	6.20	5.31
S0PP1.5	68.11	5.23	3.84	4.42	4.91	4.90	5.05	5.79	5.00
S.5PP.5	75.73	6.15	4.05	4.74	5.30	5.27	5.39	6.29	5.37
S.5PP1	74.21	6.29	4.01	4.68	5.22	5.19	5.33	6.19	5.30
S1PP.5	78.37	7.89	4.12	4.85	5.43	5.39	5.51	6.45	5.49

Table 6. Calculation of flexural parameters according to ASTM C1609 and ASTM C1018 standards.

Specimen No	Mix designs	According ASTM C1609			According ASTM C1018		
		Modulus of Rupture(MPa)	$\mathbf{T_{150}^D}$(Kj)	$\mathbf{R_{T,150}^D}$	$\mathbf{I_5}$	$\mathbf{I_{10}}$	$\mathbf{I_{15}}$
1	S0PP0	4.09	0.00	0.00	0.00	0.00	0.00
2	S.5PP0	6.25	8.06	0.54	1.75	2.50	0.00
3	S1PP0	9.15	11.45	0.52	1.75	2.63	3.05
4	S1.5PP0	10.88	14.63	0.56	1.74	2.71	3.28
5	S0PP.5	4.71	5.02	0.44	1.28	0.00	0.00
6	S0PP1	5.16	5.79	0.47	1.49	0.00	0.00
7	S0PP1.5	5.68	6.15	0.45	1.52	0.00	0.00
8	S1PP.5	6.48	11.34	0.73	1.73	2.56	2.96
9	S.5PP1	6.65	8.68	0.54	1.89	3.02	3.56
10	S.5PP.5	9.39	8.55	0.38	1.68	2.28	0.00

4.3.2. Ductility

In Table 7, the values of ductility factor of the specimens are calculated in terms of the equivalent of the displacement of the first crack and the displacement of the final crack. As shown in Table 7, the S1.5PP0 group has the most ductility factor among the specimens. The ductility factor of the S1.5PP0 group is 716, 127, and 25% higher than the S0PP0, S.5PP0, and S1PP0 groups. In samples with PP fibers, the S0PP1.5 group has the highest ductility factor. The ductility factor of the S0PP1.5 group is 87, 27, and 3% higher than the S0PP0, S0PP.5, and S0PP1 groups, respectively. Also, groups with PP fibers alone have lower ductility factor than other groups. The addition of a combination of steel and PP fibers increased the ductility factor of the specimens compared to other modes.

Table 7. Ductility of flexural specimens.

Mix designs	Max Load(KN)	Δ_y	Δ_u	Ductility
S0PP0	9.82	0.17	0.62	3.65
S.5PP0	15.01	0.40	5.25	13.13
S1PP0	21.96	0.50	11.87	23.74
S1.5PP0	26.11	0.45	13.40	29.78
S0PP.5	11.30	0.41	2.20	5.37
S0PP1	12.38	0.39	2.60	6.67
S0PP1.5	13.63	0.42	2.87	6.83
S1PP.5	15.55	0.59	12.59	21.34
S.5PP1	15.96	0.35	5.79	16.54
S.5PP.5	22.54	0.50	5.49	10.98

4.4. Impact Results

4.4.1. Impact Absorbed Energy

For all of the mix designs, the hammer has been released from a height of 600 mm. the weight of the hammer is 180 kilograms. The amount of energy that entered the specimens is 1.06kJ obtained by the specimens. This amount of energy is the result of the deformation of the specimen under impact loading. Composite samples were placed under impact loading. The force-displacement curve, peak force, crush displacement, and the energy absorbed by the specimens are obtained from the impact test. In order to make the impact tests more accurate and to plot the force-displacement curve for every specimen, three specimens were constructed and tested. The constructed specimens with various mechanical properties were placed in curing conditions. After 28 days, the specimens were tested simultaneously.

$$E = mgh = 180kg \times 9.81\ m/s\text{^}2\ \times 0.6m = 1.06kJ \quad (4)$$

After the hammer impacts the sample, first the acceleration-time curve is recorded by the machine. The acceleration suddenly changes direction and increases from the free-fall acceleration of $9.81 m/s^2$ to the impact acceleration. The equivalent value of the force impacting the specimen is obtained by the multiplication of the hammer weight (180Kg) by the acceleration values. The relationship between the impact force of the hammer and the acceleration induced follows Newton's second law. After the initial impact, the acceleration-time curve gradually lowers and approaches zero. In other words, the corresponding values of the force applied to the laboratory specimen result from the product of the acceleration curve data and the mass of the hammer. In order to calculate the force-displacement curve, the displacement values corresponding to a particular acceleration and force must be calculated. In the following, in order to plot the displacement-force curve of the specimens, velocity values are calculated in terms of

time using the Simpson numerical integration method by one-time integration of the acceleration data (Eq. 5). Displacement-time curves of the specimens are calculated in the following according to Eq. (6) by numerical integration of time-velocity data. Finally, the force-displacement curve of the samples is plotted.

$$v = (a_2 - a_1)/(t_2 - t_1) \quad (5)$$

$$x = (v_2 - v_1)/(t_2 - t_1) \quad (6)$$

The force-displacement curve of the specimens is depicted in Fig.11. As seen in the figure, the specimen with no fibers has the minimum peak force among the specimens. All specimens have reached from zero to the maximum force applied by the hammer. After the maximum force (which occurred in all specimens at the displacement below 5 mm), the force approaches zero. The displacement range is bellow 25mm in all of the specimens. In the samples with fibers, peaks of the curves increased significantly.

4.4.3. Effect of the Fibers on the Impact

To investigate the effects of the fibers on the impact parameters of disc specimens, the results of the impact test of the fiber-containing specimens should be compared to the specimens with no fibers (S0PP0). Various parameters resulting from the impact test are presented in Table 8. As can be seen, the maximum force is applied to the reference sample (without fiber), which is 38.91 KN. Also, the amount of energy absorbed by the reference sample (area under the force-displacement curve) is 188.03N.m. Also, according to the results of Table 8, the S0PP0 specimen has the greatest crush displacement. Peak force values increase with an increase in the fiber content. Maximum peak force in the specimens is related to S1.5PP0. As can be seen, the effect of steel microfibers in increasing the peak force is greater than that of PP. In the specimens containing PP fibers, the maximum force is 66.09KN (S0PP1.5 sample). The maximum force of the S1.5PP0 specimen is, respectively, 2.76 and 1.63 times higher than S0PP0 and S0PP1.5.

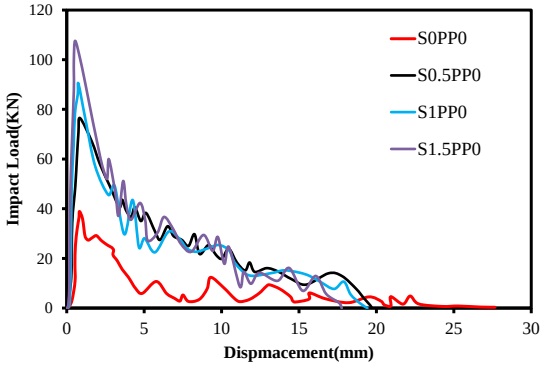

a) Only including micro steel fiber

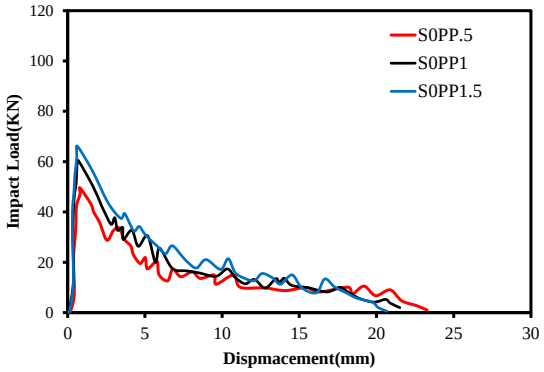

b) Only including PP fibers

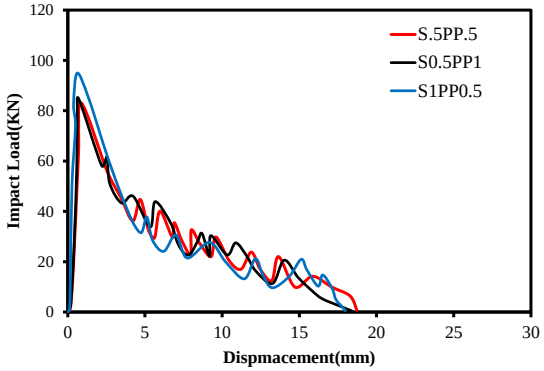

c) Including micro steel and PP fibers

Fig. 11. Force -displacement curve of all mix designs.

Table 8. Results of impact test.

Number	Specimen	Max Force (KN)	Crush Displacement (mm)	Energy Absorption (N.m)
1	S0PP0	38.91	27.66	188.03
2	S.5PP0	76.49	19.7	508.2
3	S1PP0	90.22	19.42	488.98
4	S1.5PP0	107.6	17.76	525.85
5	S0PP.5	49.53	23.28	344.48
6	S0PP1	60.36	21.51	392.44
7	S0PP1.5	66.09	20.67	443.33
8	S.5PP.5	83.08	18.73	529.24
9	S.5PP1	84.7	18.39	526.95
10	S1PP.5	94.96	17.98	534.28

4.4.4. Effect of Fibers Percentage in Failure Mode

As shown in Fig. 12, the peak force of all specimens was changed with the type of fiber. As seen in the figure, the curve is increasing for both types of fibers. The slope of the increase in the maximum force is twice in the steel fibers than the PP fibers. Also in Fig. 13, the maximum displacement for different specimens is shown in terms of fiber contents. As shown in Fig. 13, with an increase in fiber content, the crush displacement of the specimens is decreased. The decreased crush displacement of the specimens with an increase in fiber content shows increasing stiffness in the specimens. According to the Fig. 13, the specimens with steel fibers have a higher stiffness than the PP fibers. In Fig. 14, the relationship between maximum crush displacement and energy absorbed is presented. According to Fig.14, the energy absorbed is decreased with the increase of maximum crush displacemen in the all specimens.The Inverse relationship between the energy absorbed and maximum crush displacement is the result of increasing stiffness of specimens with increasing of fibers content. Fig. 15 shows the impact specimens after they have collapsed. As shown in Fig. 15, the presence of fibers in the specimens has led to the crack propagation.

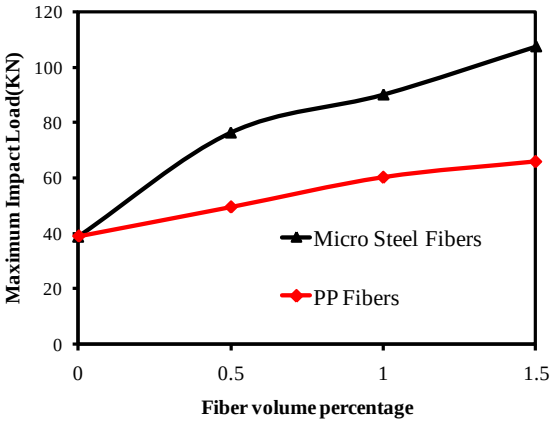

Fig. 12. Maximum Impact Load versus fiber volume fraction

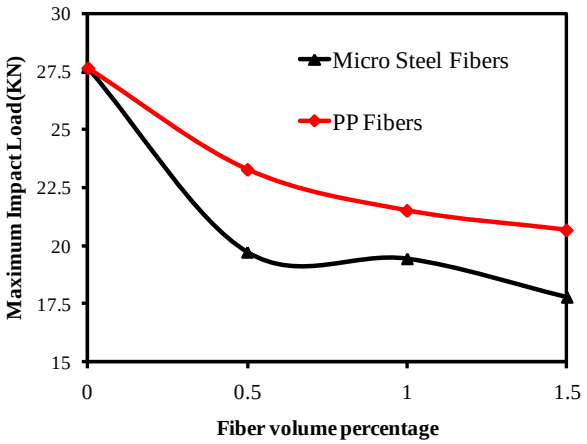

Fig. 13. Maximum crush displacement versus fiber volume fraction

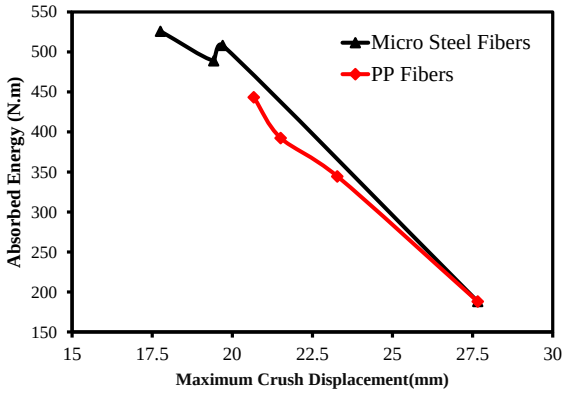

Fig. 14. Relationship between maximum crush displacement and absorbed energy

5. Conclusion and Finding

In this study, the effects of micro steel and PP fibers on mechanical properties and impact resistance of high strength cementitious composite mix designs with fine aggregates were investigated experimentally, based on 120 implemented tests. Based on the acquired test data of 120 specimens divided in 10 groups (30 cubic specimens for compressive strength, 30 beam specimens for flexural strength, 30 cylindrical 100×200mm specimens for split tensile strength and 30 disk specimens for impact resistance), the following conclusions can be drawn:

- With up to a 1% increase in the fiber content, the compressive strength of the mix designs s increased. The use of steel and polypropylene fibers higher than 1% decreases the compressive strength. With an increase in the steel fiber content from 1 to 1.5%, the compressive strength decreased by 7%. Also, with an increase in the steel fiber content from 1 to 1.5%, the compressive strength decreased by 9%.
- According to the *experimental* results, an increase in the fiber content increases the tensile strength. The tensile strength of the mix designs with fibers increased significantly compared to those without. Also according to the results, the effect of micro steel fibers on tensile strength is greater than that of polypropylene fibers. With the addition of 0.5, 1, and 1.5% of steel fibers, the tensile strength increased by 85, 130, and 186% compared to the mix designs without fibers. Also, with the addition of 0.5, 1, and 1.5% of PP fibers, the tensile strength increased by 29, 57, and 65%.
- According to the results of the flexural strength test, the maximum flexural strength is related to the S1.5PP0 group (with 1.5% microfiber steel fiber). The flexural strength of the S1.5PP0 group was 74, 166 and 19% higher than the S0PP0, S.5PP0, S1PP0 groups, respectively. Also, in groups with PP fibers, flexural strength increased with increasing fiber contents. The S0PP1.5 group had the highest flexural strength among the groups with PP fibers. The flexural strength of the S0PP1.5 group was 39, 21 and 10% higher than S0PP0, S0PP.5 and S0PP1 groups, respectively.

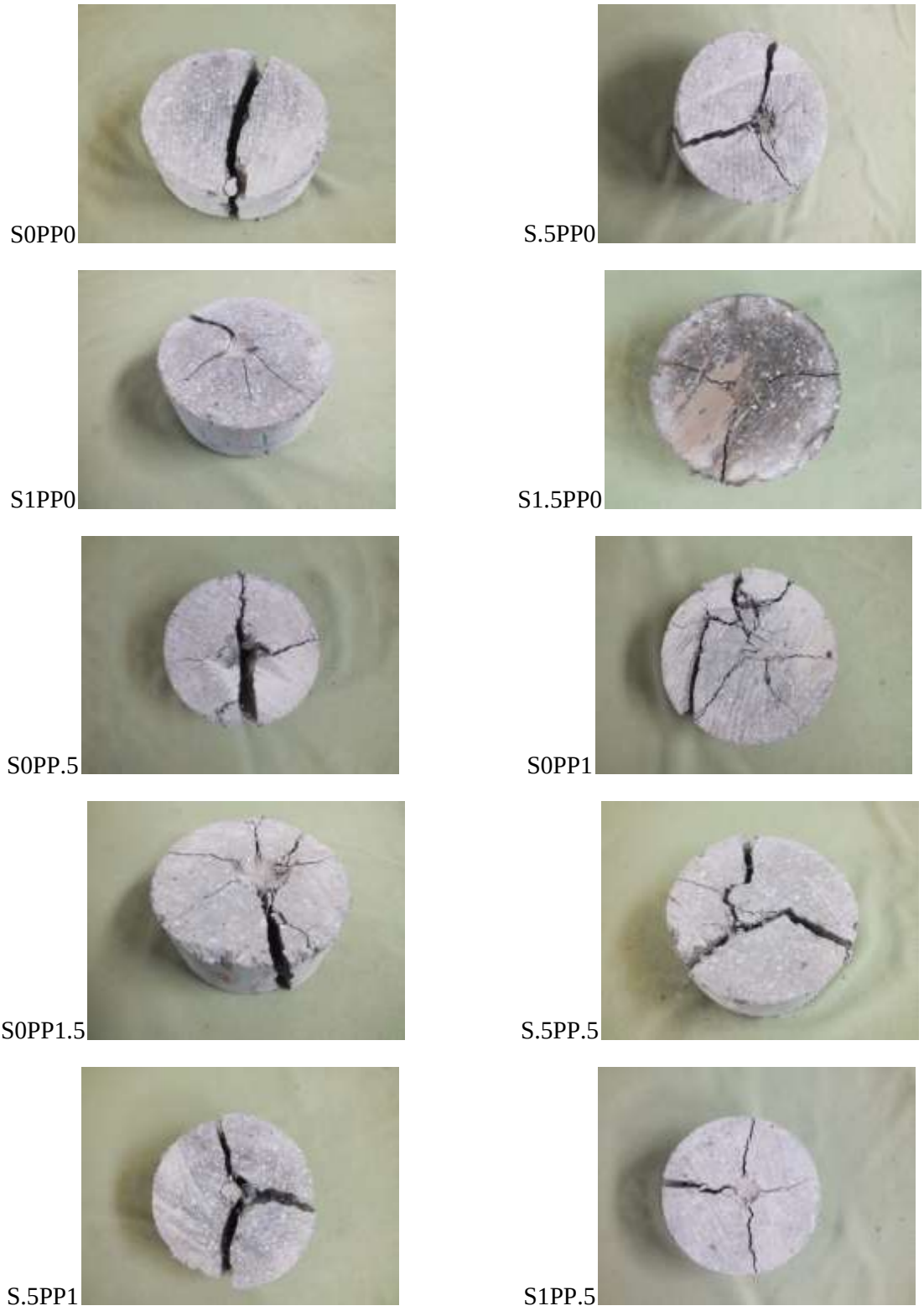

Fig 15. Failure mode of all impact specimens.

- With the increase in the fiber content, the initial peak force increases, and the crush displacement decreases. Also, the increase in initial peak force is more significant with the increase in the steel fiber content. With the increase in the micro steel fibers, the peak force increases more significantly (compared to when the same percentage of polypropylene fibers are used). Also, the use of PP fibers increases the crush displacement (compared to steel fibers). Also, according to the results, the amount of energy absorbed by the specimens with fibers increased significantly compared to those without.

REFERENCES

[1] F. U. A. Shaikh, "Review of mechanical properties of short fibre reinforced geopolymer composites," *Constr. Build.* Mater., vol. 43, pp. 37–49, 2013.

[2] M. Akinpelu and A. Adedeji, "Structural Response of Reinforced Self-Compacting Concrete Deep Beam using Finite Element Method," *Soft Comput. Civ. Eng.*, vol. 2, no. 1, pp. 36–61, 2018.

[3] C. Graczykowski, A. Orlowska, and J. Holnicki-Szulc, "Prestressed composite structures – Modeling, manufacturing, design," *Compos. Struct.*, vol. 151, pp. 172–182, 2016.

[4] A. Kheyroddin and H. Naderpour, "of Composite Rc Shear Walls," vol. 32, pp. 79–89, 2008.

[5] Garber, D., & Shahrokhinasab, E. (2019). Performance Comparison of In-Service, Full-Depth Precast Concrete Deck Panels to Cast-in-Place Decks (No. ABC-UTC-2013-C3-FIU03-Final). Accelerated Bridge Construction University Transportation Center (ABC-UTC).

[6] A. Abdelmonem, M. S. El-Feky, E. S. A. R. Nasr, and M. Kohail, "Performance of high strength concrete containing recycled rubber," *Constr. Build. Mater.*, vol. 227, p. 116660, 2019.

[7] A. S. Moghadam, F. Omidinasab, and A. Dalvand, "Experimental investigation of (FRSC) cementitious composite functionally graded slabs under projectile and drop weight impacts," *Constr. Build. Mater.*, vol. 237, p. 117522, 2020.

[8] M. Mastali, A. Dalvand, A. R. Sattarifard, Z. Abdollahnejad, and M. Illikainen, "Characterization and optimization of hardened properties of self-consolidating concrete incorporating recycled steel, industrial steel, polypropylene and hybrid fibers," *Compos. Part B Eng.*, vol. 151, no. March, pp. 186–200, 2018.

[9] M. Mastali and A. Dalvand, "Use of silica fume and recycled steel fibers in self-compacting concrete (SCC)," *Constr. Build. Mater.*, vol. 125, pp. 196–209, 2016.

[10] M. Fakharifar, A. Dalvand, M. Arezoumandi, M. K. Sharbatdar, G. Chen, and A. Kheyroddin, "Mechanical properties of high performance fiber reinforced cementitious composites," *Comput. Chem. Eng.*, vol. 71, pp. 510–520, 2014.

[11] M. Ahmadi, A. Kheyroddin, A. Dalvand, and M. Kioumarsi, "New empirical approach for determining nominal shear capacity of steel fiber reinforced concrete beams," *Constr. Build. Mater.*, vol. 234, p. 117293, 2020.

[12] D. A. Company, "Composite material," *Med. Text.*, no. JANUARY, p. 9, 2003.

[13] H. Development, "Materials Science and Engineering, 15 (1974) 31--37 ©," vol. 15, pp. 31–37, 1974.

[14] F. Recommendation, "RILEM TC 162-TDF: 'Test and design methods for steel fibre reinforced concrete' σ-ε-design method," *Mater. Struct. Constr.*, vol. 36, no. 262, pp. 560–567, 2003.

[15] A. Hemmati, A. Kheyroddin, M. Sharbatdar, Y. Park, and A. Abolmaali, "Ductile behavior of high performance fiber reinforced cementitious composite (HPFRCC) frames," *Constr. Build. Mater.*, vol. 115, pp. 681–689, 2016.

[16] L. Li, Q. Zheng, Z. Li, A. Ashour, and B. Han, "Bacterial technology-enabled cementitious composites: A review," *Compos. Struct.*, vol. 225, no. June, p. 111170, 2019.

[17] V. C. Li, "From micromechanics to structural engineering -the design of cementitious composites for civil engineering applications," *Structural Engineering/Earthquake Engineering*, vol. 10, no. 2. pp. 1–34, 1994.

[18] Ghoddousi, P., Abbasi, A. M., Shahrokhinasab, E., Abedin, M. (2019). Prediction of Plastic Shrinkage Cracking of Self-Compacting Concrete. Advances in Civil Engineering, 2019.

[19] G. Fischer, S. Wang, and V. C. Li, "Design of Engineered Cementitious Composites (ECC) for Processing and Workability Requirements," *Brittle Matrix Composites 7*. pp. 29–36, 2003.

[20] L. Wang, F. Aslani, I. Hajirasouliha, and E. Roquino, "Ultra-lightweight engineered cementitious composite using waste recycled hollow glass microspheres," *J. Clean. Prod.*, p. 119331, 2019.

[21] H. Schreiberová, P. Bílý, J. Fládr, K. Šeps, R. Chylík, and T. Trtík, "Impact of the self-healing agent composition on material characteristics of bio-based self-healing concrete," *Case Stud. Constr. Mater.*, vol. 11, 2019.

[22] L. Sun, Q. Hao, J. Zhao, D. Wu, and F. Yang, "Stress strain behavior of hybrid steel-PVA fiber reinforced cementitious composites under uniaxial compression," *Constr. Build. Mater.*, vol. 188, pp. 349–360, 2018.

[23] Sharbatdar, M. K., Abbasi, M., Fakharian, P. "Improving the Properties of Self-compacted Concrete with Using Combined Silica Fume and Metakaolin", Periodica Polytechnica Civil Engineering, 64(2), pp. 535-544, 2020. https://doi.org/10.3311/PPci.11463

[24] B. Chun and D. Y. Yoo, "Hybrid effect of macro and micro steel fibers on the pullout and tensile behaviors of ultra-high-performance concrete," *Compos. Part B Eng.*, vol. 162, pp. 344–360, 2019.

[25] V. Athiyamaan and G. Mohan Ganesh, "Experimental, statistical and simulation analysis on impact of micro steel – Fibres in reinforced SCC containing admixtures," *Constr. Build. Mater.*, vol. 246, p. 118450, 2020.

[26] Z. Abdollahnejad, A. Dalvand, M. Mastali, T. Luukkonen, and M. Illikainen, "Effects of waste ground glass and lime on the crystallinity and strength of geopolymers," *Mag. Concr. Res.*, vol. 71, no. 23, pp. 1218–1231, 2019.

[27] Q. Sun *et al.*, "Preparation and microstructure of fly ash geopolymer paste backfill material," *J. Clean. Prod.*, vol. 225, pp. 376–390, 2019.

[28] ASTM International, "Standard Specification for Portland Cement," *Annu. B. ASTM Stand.*, vol. I, no. April, pp. 1–8, 2007.

[29] G. Absorption *et al.*, "SPECIFIC GRAVITY AND ABSORPTION OF FINE AGGREGATES," pp. 1–7.

[30] ASTM International, "Standard Test Method for Compressive Strength of Cylindrical Concrete Specimens 1 This standard is for EDUCATIONAL USE ONLY .," *Annu. B. ASTM Stand.*, vol. i, no. C, pp. 1–7, 2010.

[31] ASTM C 496, "Standard Test Method for splitting tensile strength of cylindrical concrete specimen.," *Annu. B. ASTM Stand. Vol 04.02.*, pp. 1–5, 2004.

[32] Z. Keshavarz and H. Torkian, "Application of ANN and ANFIS Models in Determining Compressive Strength of Concrete ARTICLE INFO ABSTRACT," *J. Soft Comput. Civ. Eng.*, vol. 2, no. 1, pp. 62–70, 2018.

[33] C. C. Test, T. Drilled, C. Concrete, and S. T. Panels, "C 1609/C 1609M-05 Standard Test Method for Flexural Performance of Fiber-Reinforced Concrete (Using Beam With Third-Point Loading) 1," *Astm*, vol. i, no. C 1609/C 1609M-05, pp. 1–8, 2005.

[34] H. Savastano and V. Agopyan, "Transition zone studies of vegetable fibre-cement paste composites," *Cem. Concr. Compos.*, vol. 21, no. 1, pp. 49–57, 1999.

[35] A. Sadrmomtazi and A. Fasihi, "Influence of polypropylene fibers on the performance of nano-SiO 2-incorporated mortar," *Iran. J. Sci. Technol. Trans. B Eng.*, vol. 34, no. 4, pp. 385–395, 2010.